Biomechanics of Calcaneus Impacted by Talus: A Dynamic Finite Element Analysis

Mengquan Huang
Southern Medical University
Bin Yu (420229872@qq.com)
Southern Medical University
Yubiao Li
Air Force Hospital of Southern Theater Command of PLA
Chunlai Liao
Air Force Hospital of Southern Theater Command of PLA
Jun Peng
Air Force Hospital of Southern Theater Command of PLA
Naiming Guo
Air Force Hospital of Southern Theater Command of PLA

Research

Keywords: calcaneal fracture, biomechanics, talus, explicit dynamic, finite element

Posted Date: June 21st, 2021

DOI: https://doi.org/10.21203/rs.3.rs-600528/v1

Abstract

Background

The biomechanics of calcaneus impacted by the talus are unclear. We aimed to evaluate the biomechanical effect of the talus impacting on the calcaneus at different falling speed, and analyze the factors affecting calcaneal fracture.

Methods

A finite element model including the talus, calcaneus and ligaments was built using a variety of three-dimensional reconstruction software. The method of explicit dynamics was used to analyze the process of the talus impacting the calcaneus. Stress values of the posterior, middle, and anterior subtalar articular surface(PSAS, ISAS, ASAS), the calcaneocubic articular surface(CAS), the bottom of the calcaneus(BC), the medial wall (MW)and lateral wall (LW) of the calcaneus were extracted. Stress quantity and distribution changes in various parts of the calcaneus changed with speed were analyzed.

Results

Posterior subtalar articular surface reached the peak stress first during the process of talus impacting the calcaneus. The stress was mainly concentrated on the PSAS, ASAS, MW and GA. Comparing with the speed of 5m/s, the average maximum stress increased in each region of the calcaneus were: PSAS 73.81%, ISAS 7.11%, ASAS 63.57%, GA 89.10%, LW 140.16%, CAS 140.58%, BC 137.67%, MW 135.99% at a speed of 10m/s. The regions where the stress were concentrated changed, and the magnitude and sequence of stress peaks of calcaneus changed with speed also during the impact.

Conclusion

The falling speed affected the value and distribution of stress of the calcaneus, which was the most important factor leading to a calcaneal fracture. The magnitude and sequence of stress peaks might be important factors in determining the beginning and direction of fracture lines.

Background

Calcaneal fractures account for nearly one-third of foot injuries. Falling is the most common cause of this type of injury [1]. Understanding injury mechanisms and injury patterns is crucial to the decision-making of surgery [2]. Due to the complex anatomy, lack of blood vessels, weight-bearing and continuous movement, the treatment of calcaneal fractures is very costly. Patients may be completely disabled for up to 3 to 5years [3].

Axial compression load was the main cause of hindfoot fractures [4]. The impact of the talus on the calcaneus was the direct factor leading to the calcaneal fracture. At present, most studies on cadaver specimens were loaded with impact speed or energy, and tested through high axial compression loads to produce calcaneal fractures [5–7]. In the study of Carr et al.[6], 18 cadaveric tibial specimens were loaded at different speed to create models of intra-articular calcaneal fracture. It found that calcaneal fractures were composed of two basic fracture lines. One basic fracture line divided the calcaneus into inside and outside parts, and the fracture line extended to the calcaneocubic joint and the anterior subtalar articular surface. Another basic fracture line divided the calcaneus into anterior and posterior parts, extending from the Gissane angle to the medial wall of calcaneus. Essex-Lopresti et al. [7] believed that the primary calcaneal fracture line was initially formed between the lateral process of the talus and the lateral edge of the calcaneus. The lateral wall of the calcaneus and the body of the calcaneus was separated at the Gissane angle. And then an anterolateral fracture, or a compression fracture of the articular surface, or a tongue-shaped fracture of the calcaneus was formed. However, these analyses of calcaneal fracture patterns were the results of direct observation from experiments, and there were still some controversies.

At present, stress change of the calcaneus impacted by the talus at different speed was still unclear. There was no report on these biomechanical changes. The method of finite element analysis could visually display the amount and distribution of

stress in various regions of the calcaneus.[8] It could help us understand the process of calcaneal fractures.

In this study, a finite element model consisting of talus and calcaneus would be constructed. The explicit dynamics method was used to analyze the mechanical changes of the calcaneus. The aim of this study was to evaluate the mechanical effect of the talus impacting on the calcaneus at different falling speed, and analyze the factors affecting calcaneal fracture.

Material And Methods

Model construction

A healthy male volunteer (24 years old; height, 172cm; weight, 65.3kg) without heel deformities and no history of fractures by X-ray examination was selected as the subject of this study. This study was approved by the ethics committee of our hospital. A patient’s informed consent was obtained. The volunteer's left ankle was scanned with a spiral computerized tomography (CT) machine. The ankle was set at the neutral position. The scan range was from the bottom of the heel to 10cm above the ankle joint. The slice thickness was 0.625mm. CT images stored in Dicom format were segmented in the software of Mimics (version 10.0, Materialise, Belgium) to create three- dimensional (3D) images of the calcaneus and talus. The 3D image was optimized to form a high-quality non-uniform rational B-splines (NURBS) surface using the software of Geomagic Studio (version 12.0, Geomagic company, America). The calcaneus and talus were assembled in the neutral position according to the anatomic in the software of Solidworks (version 2010, Solidworks, France). The cortical bone and cancellous bone are divided in the software of Ansys Workbench (version 14.0, Ansys Inc, America). According to the anatomical position, the posterior talocacane ligament, the medial talocacane ligament, the lateral talocacane ligament and the intertalar calcaneus ligament were established.

Material properties

According to the setting method of previous studies, the elastic modulus and Poisson's ratio of cortical bone were set to 7.5GPa and 0.3, respectively. The elastic modulus and Poisson's ratio of cancellous bone were set to 400MPa and 0.3, respectively. Both the bones were set as isotropic material [9]. The material properties of human ligaments had nonlinear characteristics. But the ligaments were often simplified as elastic isotropic in most of researches. The ligament was set as an isotropic linear beam, and the elastic modulus and Poisson's ratio of the were set to 80MPa and 0.40 [10].

Boundary and initial condition

The talus was loaded with an initial speed of 5m/s, 6m/s, 7m/s, 8m/s, 9m/s and 10m/s, respectively. The loading direction was vertical downward. The calcaneal tuberosity and the calcaneocubic joint surface were totally constrained. The talus was set as a rigid body. The end time was 1.5ms. The analysis type was explicit dynamics, and the solver was autodyn.(Fig. 1)

Data analysis

Two to six nodes of the posterior subtalar articular surface (PSAS), the intermediate subtalar articular surface (ISAS), the anterior subtalar articular surface (ASAS), the Gissane angle (GA), the lateral wall (LW), the medial wall (MW), the calcaneocubic articular surface (CAS) and the bottom of the calcaneus (BA) were used to analyze the stress changes. (Fig. 2A, B, C) The maximum von-Mises stress value of these nodes during the end time was extracted to evaluate the stress changes in each region of the calcaneus. The datum was expressed in the form of mean ± standard deviation ($\bar{x}\pm s$). Repeated measures analysis of variance was used for data analysis. One point of each region was chosen to analyze the relationship between stress and time (Fig. 2A, B, C). $P < 0.05$ indicates that the difference was statistically significant. The SPSS 13.0 software was utilized to perform statistical analysis.

Results

Using three-dimensional reconstruction software and finite element analysis software, a model containing of the talus, calcaneus, and ligaments was constructed. The model had a good geometric similarity with the actual bone and ligaments. There was a total of 10084 nodes and 30686 elements in the model. The distribution cloud diagram and the value of maximum stress of each region of the calcaneus under different initial conditions were obtained.

With the increase of the impact velocity of the talus, the stress value of each region of the calcaneus increased, and the magnitude of the increase of the stress was different. The average maximum stress results of each region were shown in Table 1. Under different impact velocities of the talus, the mean maximum stresses of the PSAS, LW, CAS, BA, and MW had statistically significant differences (P values were 0.024, 0.004, < 0.001, < 0.001, 0.001, respectively). The mean maximum stress of the ISAS, ASAS and GA was not statistically significant (P values were 0.289, 0.213, 0.087, respectively). When the speed of talus was 10m/s, compared to 5m/s, the average maximum stress increased in each region of the calcaneus were: PSAS 73.81%, ISAS 7.11%, ASAS 63.57%, GA 89.10%, LW 140.16%, CAS 140.58%, BC 137.67%, MW 135.99%. The area of high stress changed with the different speed. (Fig. 3)

Discussion

Foot and ankle injuries were usually caused by high energy falls in many people [11]. People who were healthy and active had a higher risk of falling. Because they might perform more dangerous activities, such as climbing ladders to roofs [2]. The heel drop was a rather quick process. During this process, there was a considerable reaction force between the foot and the ground. Studies had found that this force was about 8 to 14 times the body weight of the human body [12]. When the impact load exceeded the endurance limitation of the human musculoskeletal system, damage would occur. Researching the biomechanics of the calcaneus during this process was critical for understanding the mechanism of high energy trauma in the hind foot.

The main finding of this study was that with the increase of the velocity, the amplitude of the stress increased in each area of the calcaneus and the location of the stress concentration changed. The speed when the foot falling to the ground was related to the height of the fall, which determined the impact load at the heel when landing [13]. The impact velocity of the foot during walking and running was between 0.52 m/s and 0.72 m/s [14]. In sports such as skiing, impact velocity might reach 14.0 m/s at a drop height of 10 meters [15]. Funk et al. [16] found that about 93% of the specimens had calcaneal fractures under an impact of 5.0 m/s. This study found that with the increase of the impact velocity of the talus, the stress of the calcaneus also increased significantly. The stress of the medial wall, lateral wall and calcanecubic joints increased the most. Falling speed was the most important factor leading to calcaneal fractures. For every 1m/s increased in speed, the stress of each area of the calcaneus could increase by about 50% at most. Therefore, reducing the influence of the talus on the calcaneus during a fall was the principal way to reduce calcaneal fractures.

Yoganandan et al. [17] simulated the intra-articular and extra-articular fractures of the calcaneus by applying axial loads on the feet of the cadaver specimen, and conducted experimental studies on the loads required to produce calcaneal fractures. It turned out that the greater the loads, the easier the damage was the calcaneus. Another study had shown that axial compression was dominant in calcaneal fractures, and as the impact speed increased, the chance of calcaneal injury increased[5]. However, stress changes of the calcaneus were not reported in these studies. This study performed a quantitative analysis. The results of this study reflect the relationship between the speed and stress of various regions of the calcaneus, as well as the relationship between the stress and time. With increasing the speed of the talus, the stress increasing in various regions were not consistent due to the anatomical characteristics of the calcaneus. This resulted in different areas of calcaneal fractures at different speed. Therefore, calcaneal fracture lines were diverse.

Another finding of this study was that the initial positions of calcaneal fractures might be related to the sequence of stress peaks. There were still many controversies about the various position and direction of fracture lines, even primary fracture lines [16, 18]. The comminution and displacement of calcaneal fractures, and the combination of various fracture lines produced various fracture morphology. The study of Utheza et al. [19] believed that the main fracture line was variable, but

always centered on the sustentaculum tali. Warrick et al. [20] believed that the fracture line extended forward and outward from a point on the medial wall of the calcaneus to various positions behind the sustentaculum tali. In this study, we found stress concentrations in the posterior, anterior, and intermediate subtalar joints, the medial wall, and the Gissane angle. These stress concentration locations were basically the same as the locations of fracture in the model proposed by Carr et al. [6]. Obviously, when the stress peak appeared early and the regional stress exceeded the limit load of the bone, the starting point of the calcaneal fracture might appear at this time. As the stress concentration areas of the calcaneus increased, the sites of possible fracture increased, which led to compound fracture lines.

There were some shortcomings in this study. First of all, the forefoot, midfoot and heel soft tissues were not created in this study. In fact, the soft tissues of the foot and many joints could absorb energy. The damping properties of muscles, skin and cartilage could reduce the stress, transfer and consume high energy generated by the impact process. However, these factors did not affect the mechanical characteristics of the talus on the calcaneus. Secondly, the human weight was not applied to the calcaneus. The results obtained could roughly reflect the calcaneal stress distribution and the degree of change, but the conclusions have limitations. In fact, impact injury of the calcaneus was a very complicated process. A more accurate finite element model, more precise material properties and boundary conditions were needed in order to make the simulation technology closer to reality. More research will be needed in the future.

Conclusions

The falling speed affected the value and distribution of stress of the calcaneus, which was the most important factor leading to a calcaneal fracture. With the increase of the impact velocity of the talus, the stress of each area of calcaneus increased. Locations of calcaneal stress concentration were posterior, intermediate, and anterior subtalar joints, Gissane angle and medial wall. The magnitude and sequence of stress peaks might be important factors in determining the beginning and direction of fracture lines.

Declarations

Ethics approval and consent to participate: Yes

Consent for publication: Yes

Availability of data and material: Not applicable

Competing interests: Not applicable

Funding: Not applicable

Authors' contributions:

Yu B contributed to the study conception and design. Material preparation, data collection and analysis were performed by Huang M, Li Y, Liao C, Peng J, Guo N. The first draft of the manuscript was written by Huang M and all authors commented on previous versions of the manuscript. All authors read and approved the final manuscript.

Acknowledgments

The software used in this study was authorized by the Anatomy Laboratory of Southern Medical University.

References

1. Herrera-Pérez M, Oller-Boix A, Valderrabano V, et al. Calcaneal fractures: controversies and consensus. Acta Ortop Mex. 2018;32(3):172–81.

2. Galluzzo M, Greco F, Pietragalla M, et al. Calcaneal fractures: radiological and CT evaluation and classification systems. Acta Biomed. 2018;89(1-S):138–50.
3. Clare MP, Crawford WS. Managing complications of calcaneus fractures. Foot Ankle Clin. 2017;22(1):105–16.
4. Stephens AR, Grujic L. Post-Traumatic hindfoot arthritis. J Orthop Trauma. 2020;34(Suppl 1):32–7.
5. Gallenberger K, Yoganandan N, Pintar F. Biomechanics of foot/ankle trauma with variable energy impacts[J]. Ann Adv Automot Med. 2013;57:123–32.
6. Carr JB, Hamilton JJ, Bear LS. Experimental intra-articular calcaneal fractures: anatomic basis for a new classification[J]. Foot Ankle. 1989;10(2):81–7.
7. Essex-Lopresti P. The mechanism, reduction technique, and results in fractures of the os calcis[J]. Br J Surg. 1952;39(157):395–419.
8. Tsubone T, Toba N, Tomoki U, et al. Prediction of fracture lines of the calcaneus using a three-dimensional finite element model[J]. J Orthop Res. 2019;37(2):483–9.
9. Wang Y, Wong DW, Zhang M. Computational models of the foot and ankle for pathomechanics and clinical applications: A review[J]. Ann Biomed Eng. 2016;44(1):213–21.
10. Wang Y, Li Z, Wong DW, et al. Effects of ankle arthrodesis on biomechanical performance of the entire foot[J]. PLoS One,2015,10(7):e134340.
11. Snoap T, Jaykel M, Williams C, Roberts J. Calcaneus fractures: A possible musculoskeletal emergency. J Emerg Med. 2017;52(1):28–33.
12. Mcnitt-Gray LJ. Kinematics and impulse characteristics of drop landings from three heights [J]. Int J Sport Biomech. 1991;7(2):201–24.
13. Mcnitt-Gray JL. Kinetics of the lower extremities during drop landings from three heights[J]. J Biomech,1993,26(9):1037–1046.
14. Chi KJ, Schmitt D. Mechanical energy and effective foot mass during impact loading of walking and running[J]. J Biomech. 2005;38(7):1387–95.
15. M H. Safer Ski jump landing surface design limits normal impact velocity. Skiing trauma and safety.[J]. 2019,17.
16. Funk JR, Crandall JR, Tourret LJ, et al. The axial injury tolerance of the human foot/ankle complex and the effect of Achilles tension[J]. J Biomech Eng. 2002;124(6):750–7.
17. Yoganandan N, Pintar FA, Seipel R. Experimental production of extra- and intra-articular fractures of the os calcis[J]. J Biomech. 2000;33(6):745–9.
18. Miric A, Patterson BM. Pathoanatomy of intra-articular fractures of the calcaneus[J]. J Bone Joint Surg Am,1998,80(2):207–212.
19. Utheza G, Goldzak M, Chaminade B, et al. 3-dimensional imaging of thalamic fractures of the calcaneum. Validation of classifying fractures into 3 forms[J]. Rev Chir Orthop Reparatrice Appar Mot,1998,84(5):440–450.
20. Warrick CK, Bremner AE. Fractures of the calcaneum, with an atlas illustrating the various types of fracture[J]. J Bone Joint Surg Br,1953,35-B(1):33–45.

Tables

Table1 The mean maximum stress of each region of the calcaneus during a 5-10m/s drop. ($\bar{x}\pm s$, MPa)

	5m/s	6m/s	7m/s	8m/s	9m/s	10m/s	P-value
PSAS	9.283±4.268	10.468±4.848	12.038±5.587	13.01±6.079	15.44±7.193	16.135±7.564	0.024*
ISAS	10.153±5.674	10.89±5.188	10.492±4.621	9.727±3.522	8.852±3.045	10.875±3.8745	0.289
ASAS	11.062±2.518	12.348±5.469	13.416±5.576	15.971±6.367	16.7±5.632	18.094±4.646	0.213
GA	6.826±0.935	10.23±1.292	10.991±1.338	11.572±1.616	12.383±2.164	12.908±1.194	0.087
LW	3.312±0.825	4.216±0.565	4.688±0.704	5.415±0.384	5.83±1.048	7.945±1.445	0.004*
CAS	4.956±0.259	6.198±0.401	7.892±0.450	9.539±0.895	11.565±1.079	11.923±0.649	<0.001*
BC	2.931±0.376	3.788±0.413	4.594±0.635	5.761±0.652	6.016±1.276	6.966±1.155	<0.001*
MW	5.567±0.528	7.152±0.573	8.868±0.661	9.633±1.904	11.617±2.313	13.138±2.812	0.001*

Note: Posterior subtalar articular surface (PSAS), intermediate subtalar articular surface (ISAS), anterior subtalar articular surface (ASAS), Gissane angle (GA), lateral wall (LW), medial wall (MW) , calcaneocubic articular surface (CAS), bottom of the calcaneus(BC). * P<0.05, statistically significant.

Table 2 The sequence of the maximum stress of each calcaneal region at different speed.

Speed			Sequence of peak stress		
5m/s	PSAS	CAS, MW	ASAS, ISAS	GA	LW, BC
6m/s	PSAS	CAS	ASAS, MW	ISAS, GA	LW, BC
7m/s	PSAS	ASAS, MW, CAS	ISAS, GA	BC, LW	
8m/s	PSAS	CAS	ASAS, MW	ISAS, GA	LW, BC
9m/s	PSAS	ISAS	CAS, MW	ASAS, GA	BC , LW
10m/s	PSAS, ISAS	ISAS, MW, CAS	GA	BC, LW	

Note: Posterior subtalar articular surface (PSAS), intermediate subtalar articular surface (ISAS), anterior subtalar articular surface (ASAS), Gissane angle (GA), lateral wall (LW), medial wall (MW) , calcaneocubic articular surface (CAS), bottom of the calcaneus(BC).

Figures

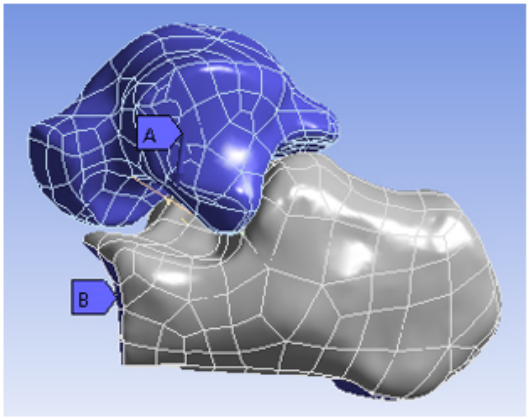

Figure 1

Finite element model with boundary conditions. A, Velocity. B. Fixed support.

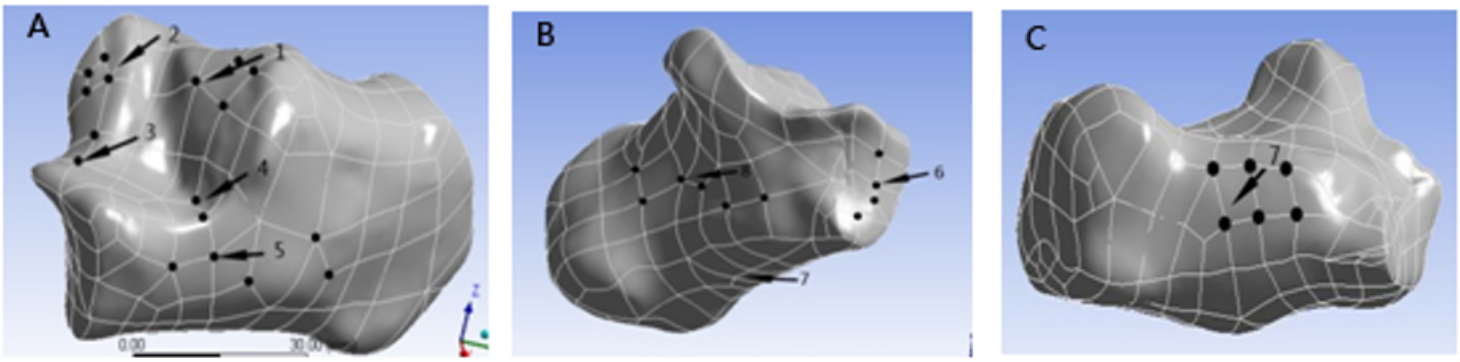

Figure 2

Select the nodes in each region to extract the stress of the calcaneus (A, B, C). Seven nodes were selected to analyze the stress changing with the time (Number1 to 7 in A, B and C).

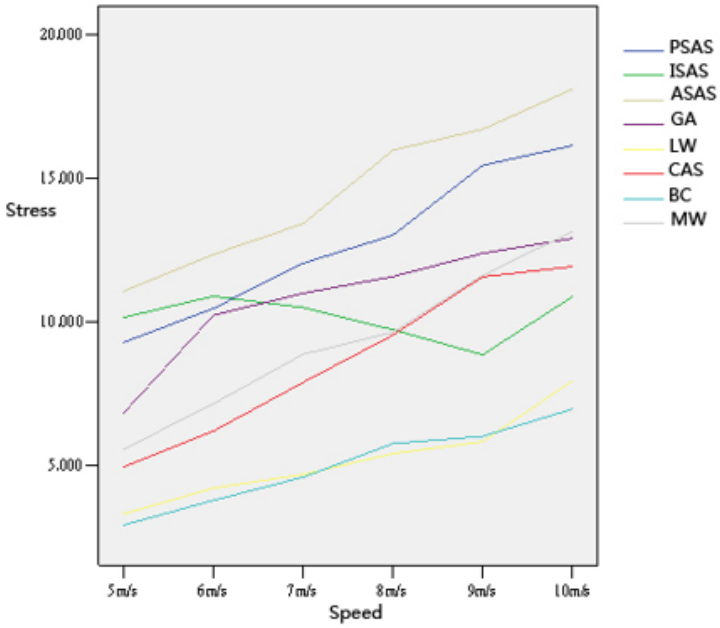

Figure 3

Mean maximum stress in each region of the calcaneus at different speed.

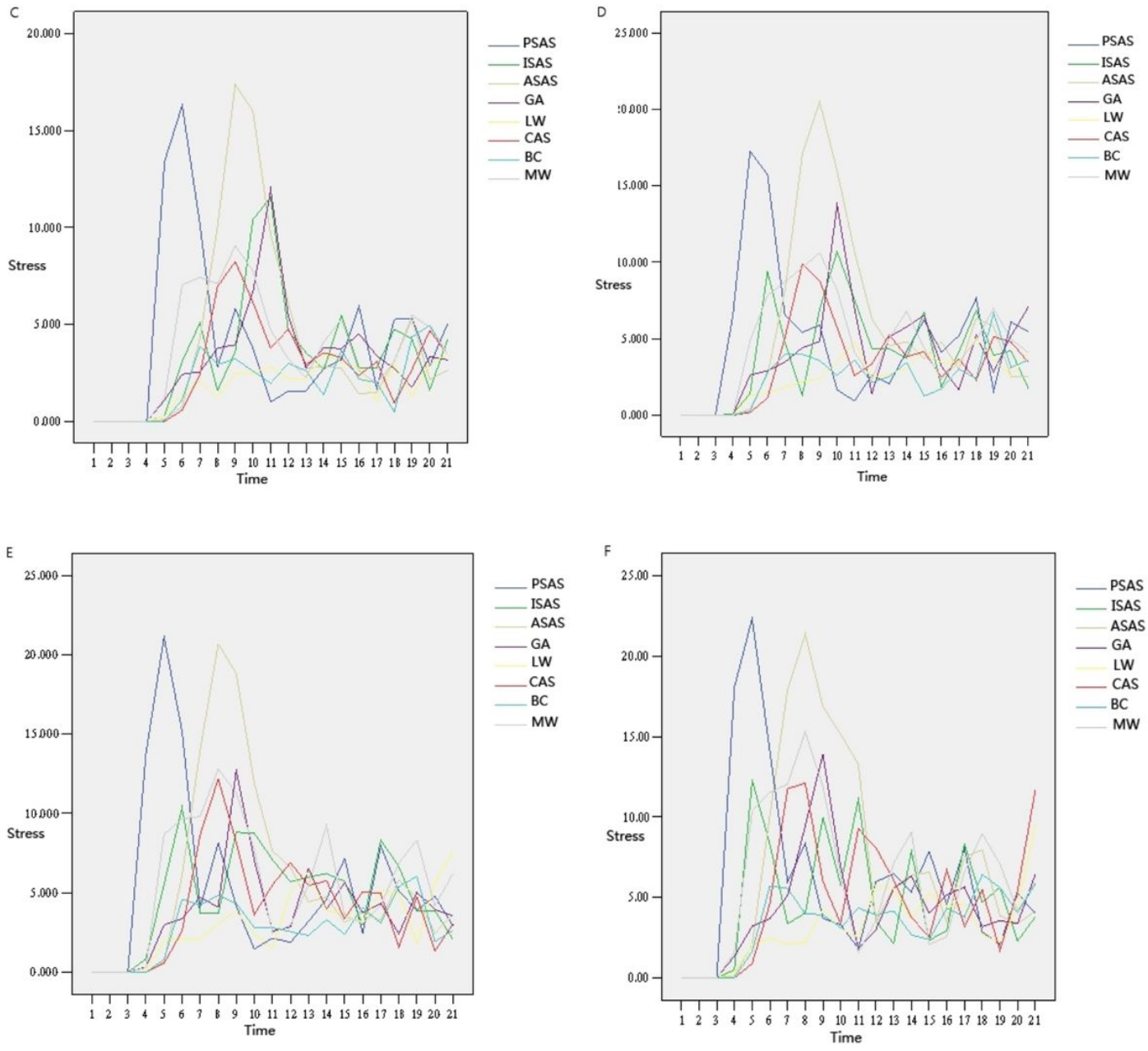

Figure 4

Stress of the calcaneus changed with speed during 1.5ms. A, 5m/s. B, 6m/s. C, 7m/s. D, 8m/s. E, 9m/s. F, 10m/s.

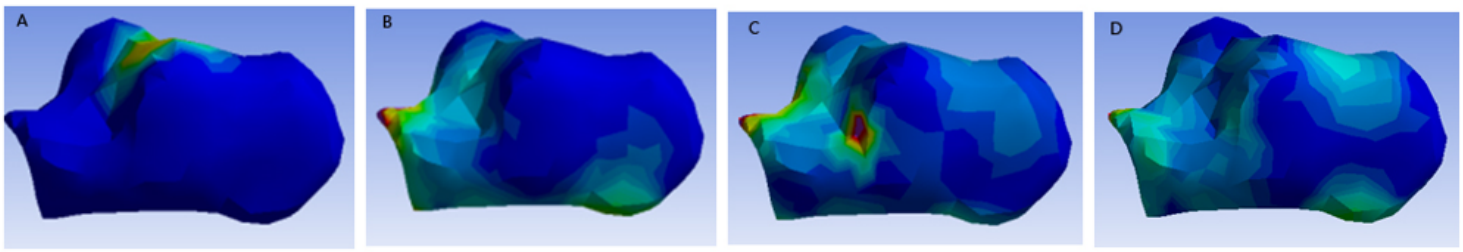

Figure 5

Stress distribution of the calcaneus during a 10m/s drop at different moment. A, 0.25863ms. B, 0.41381ms. C, 0.56899ms. D, 0.82762ms.